Volume 39
Number 2
January 24, 2000

Inorganic Chemistry

Articles

Direct Determination of the Single-Ion Anisotropy in a One-Dimensional Magnetic System by High-Field EPR Spectroscopy; Synthesis, EPR, and X-ray Structure of $Ni_xZn_{1-x}(C_2O_4)(dmiz)_2$ [$x = 0.07$]

Luca A. Pardi,*[†,‡] Alia K. Hassan,[†,§] Frans B. Hulsbergen,[||] Jan Reedijk,*[||] Anthony L. Spek,[⊥] and Louis-Claude Brunel[†]

National High Magnetic Field Laboratory, 36302 Tallahassee, Florida, Leiden Institute of Chemistry,
Gorlaeus Laboratories, Leiden University, P.O. Box 9502, 2300 RA Leiden, The Netherlands,
Bijvoet Center for Biomolecular Research, Crystal and Structural Chemistry, Utrecht University,
Padualaan 8, 3584 CH Utrecht, The Netherlands, and Grenoble High Magnetic Field Laboratory,
Max-Planck-Institut für Festkörperforschung and Centre National de la Recherche Scientifique,
BP 166, 38042 Grenoble Cedex 09, France

Received February 10, 1999

The synthesis, X-ray structure, and EPR measurements of the integer-spin linear-chain antiferromagnet [Ni(ox)(dmiz)$_2$] (where ox = $C_2O_4^{2-}$ and dmiz = 1,2-dimethylimidazole) are presented. The sign and size of the single-ion zero field splitting (Zfs) of the divalent Ni have been determined by high field/high-frequency EPR spectroscopy. The spectra of powder samples of the derivatives [$Ni_xZn_{1-x}(C_2O_4)(dmiz)_2$] for $x = 0.09$ and 0.07, at frequencies ranging from 110 to 440 GHz allowed the accurate determination of the zfs parameters D and E, with $D = 1.875(4)$ cm^{-1} and $E = 0.38$ cm^{-1}. The X-ray structure has been determined from measurements on a single crystal with $x = 0.07$. Structural parameters are as follows: $a = 14.5252(7)$ Å, $b = 12.1916(8)$ Å, $c = 8.6850(8)$ Å, $\beta = 97.460(6)°$ in space group $C2/c$. The zigzag chain contains octahedrally coordinated metal ions with two cis-oriented N-coordinated dmiz ligands and two cis-oriented, tetradentate bridging oxalato(2−) ligands, together resulting in a MN_2O_4 donor set. The structure was refined to a conventional R value of 0.073 for 1051 observed reflections. Zn−O distances are 2.167(5) Å and Zn−N = 2.098 Å. Coordination angles vary for cis angles from 78.4 to 100.7°, with trans angles varying from 163.9° to 165.5°.

Introduction

The study of the magnetism of one-dimensional materials has recently received a new impulse from the synthesis of a number of linear chain compounds of Ni(II) and from the investigation of their magnetic properties.[1−14] These compounds were prepared with the aim of realizing a quantum integer-spin antiferromagnetic chain.

[†] National High Magnetic Field Laboratory.

[‡] Present address: Istituto Fisica Atomica e Molecolare, Consiglio Nazionale delle Ricerche, via del Giardino 7, 56127, Pisa, Italy.

[§] Max-Planck-Institut für Festkörperforschung and Centre National de la Recherche Scientifique.

[||] Leiden University.

[⊥] Utrecht University.

(1) Chou, L.-K.; Abboud, K. A.; Talham, D. R. *Chem. Mater.* **1994**, *6*, 2051.
(2) Deguchi, H.; Takagi, S.; Ito, M.; Takeda, K. *J. Phys. Soc. Jpn.* **1995**, *64*, 22.
(3) Goto, T.; Sato, S.; Kitamura, K.; Fujiwara, N.; Renard, J. P.; Meisel, M. W. *J. Magn. Magn. Mater.* **1998**, *177*, 663.
(4) Granroth, G. E.; Chou, L. K.; Kim, W. W.; Chaparala, M.; Naughton, M. J.; Haanappel, E.; Lacerda, A.; Rickel, D.; Talham, D. R.; Meisel, M. W. *Physica B* **1995**, *211*, 208.
(5) Granroth, G. E.; Maegawa, S.; Meisel, M. W.; Krzystek, J.; Brunel, L. C.; Bell, N. S.; Adair, J. H.; Ward, B. H.; Fanucci, G. E.; Chou, L. K.; Talham, D. R. *Phys. Rev. B: Condens. Matter* **1998**, *58*, 9312.
(6) Ito, M.; Yamashita, H.; Kawae, T.; Takeda, K. *J. Magn. Magn. Mater.* **1998**, *177*, 673.
(7) Katsumata, K.; Hori, H.; Takeuchi, T.; Date, M.; Yamagischi, A.; Renard, J. P. *Phys. Rev. Lett.* **1989**, *63*, 86.
(8) Koido, N.; Kambe, T.; Teraoka, S.; Hirai, S.; Goto, T.; Chou, L.-K.; Talham, D. R.; Meisel, M. W.; Nagata, K. *J. Magn. Magn. Mater.* **1995**, *140−144*, 1639.

10.1021/ic990167x CCC: $19.00 © 2000 American Chemical Society
Published on Web 01/04/2000

According to the Haldane conjecture,[15] the properties of the ground state and of the low-energy excitations of a one-dimensional Heisenberg antiferromagnet are different for integer and half-integer spins. For the systems with integer spin, a gap exists between the disordered nonmagnetic spin-singlet ground state and the first excited triplet state at the bottom of the excited band of states. In contrast, the systems with half-odd-integer spin should remain gapless. The Haldane conjecture is, as the word suggests, a supposition still to be proved or disproved. Recent theoretical and experimental investigations have put this subject on a more firm basis and confirmed the existence of an energy gap in integer-spin chains. Moreover it is clear that this is an effect that has a combined quantum mechanical and many-body nature,[16−19] to be distinguished, for example, from the purely quantum mechanical origin of spin gap in discrete spin clusters.

In this frame, coordination chemistry has played a central role making available to experimentalists and theoreticians a considerable number of linear chain compounds in which Ni(II) ions are bridged by a variety of molecules.[1,20,21] The study of the magnetism of these system as well as that of the inorganic analogue[9,22] Y_2BaNiO_5 confirmed the existence of the singlet−triplet energy gap, as stated by the Haldane conjecture.

In general the magnetic properties of these systems are interpreted using a spin Hamiltonian of the form given in eq 1:

$$\mathbf{H} = \sum J S_i S_j + \sum D[S_{iz}^{\ 2} - S(S+1)/3] + E(S_{ix}^{\ 2} - S_{jy}^{\ 2}) \quad (1)$$

where i and j are limited to nearest neighbor sites and J is the exchange coupling constant between the $S = 1$ spins of the nearest neighbor Ni(II) ions and D and E are the zero field splitting (zfs) parameters. Electron paramagnetic resonance (EPR) spectroscopy offers the possibility to have a direct measurement of the zfs, but there are a series of problems to face: (i) the one-dimensional system under study is magnetically nondiluted. It contains an infinite number of exchange-coupled magnetic ions which make the observation of the zfs of the single ion not amenable. In principle the zfs of the excited triplet above the Haldane gap may be observed,[23] but its sign and size are not trivially related to the single ion zfs unless some simplifying assumptions are made.[24] In particular, assuming uniform exchange coupling along the chain results in a D parameter of the spin triplet which is equal to that of the single ion, unless some exchange and/or dipolar anisotropy is operative, and (ii) in the case of divalent Ni, the zfs ranges from a few[25] to some tens of wavenumbers,[26,27] and conventional X- and Q-band EPR spectroscopy, using electromagnetic quanta around 0.3 and 1.5 cm^{-1}, respectively, may fail to excite transitions between the states of the spin triplet manifold. From this point of view high-frequency/high-field EPR offering radiation quanta ranging from 2.5 cm^{-1} (75 GHz) to 18 cm^{-1} (550 GHz) and higher, corresponding to the millimeter and submillimeter band of the electromagnetic spectrum, is a valuable tool.[28]

Several years ago one of the authors synthesized and characterized a series of one-dimensional compounds of formula *cis*-$[M(C_2O_4)L_2]$ (MOxim), where M is a divalent first-transition series metal ion and L is an imidazole ligand.[29] The structure of such a class of compounds appears to be a zigzag chain, as redrawn in Figure 1 for a representative example determined in the present study. All such compounds do show a clear one-dimensional structure. The Ni(II) derivatives are thus very good candidates for the study of the Haldane problem. In fact, at the time of their first appearance in the literature, the Haldane conjecture was not made yet, and only recently these systems have been revisited with the new aim of studying the Haldane system.[30,31] An interesting property of the MOxim family is the fact that they can be doped with Zn(II) in any desired ratio.[29] This fact offers the possibility to measure the zfs of the Ni(II) single ion in the same environment as in the pure sample, by measuring EPR spectra of the $Ni_xZn_{1-x}(C_2O_4)L_2$ compounds for low values of x at which the isolated Ni(II) ion are statistically prevalent relative to dimers and other higher nuclearity clusters. The study presented in this paper allowed us to determine directly the size and the sign of the zfs parameters of the Ni(II) in the chain. This is, to our knowledge, the first report of the direct measurement of the single-ion zfs

---

[9] Ramirez, A. P.; Cheong, S.-W.; Kaplan, M. L. *Phys. Rev. Lett.* **1994**, *72*, 3108.

[10] Renard, J. P.; Verdaguer, M.; Regnault, L. P.; Erkelens, W. A. C.; Rossat-Mignod, J.; Stirling, W. G. *Europhys. Lett.* **1987**, *3*, 945.

[11] Shiba, H.; Sakai, T.; Luthi, B.; Palme, W.; Sieling, M. *J. Magn. Magn. Mater.* **1995**, *140−144*, 1590.

[12] Sieling, M.; Palme, W.; Luthi, B.; Brill, T. M.; Boucher, J. P.; Renard, J. P. *J. Magn. Magn. Mater.* **1995**, *140−144*, 1637.

[13] Sieling, M.; Rieth, T.; Schmidt, S.; Luthi, B.; Zvyagin, S. A. *J. Magn. Magn. Mater.* **1998**, *177*, 695.

[14] Zaliznyak, I. A.; Dender, D. C.; Broholm, C.; Reich, D. H. *Phys. Rev. B: Condens. Matter* **1998**, *57*, 5200.

[15] Haldane, F. D. M. *Phys. Rev. Lett.* **1983**, *50*, 1153.

[16] Afflek, I. *J. Phys. Condens. Matter* **1989**, *1*, 3047.

[17] Afflek, I. *Phys. Rev. B: Condens. Matter* **1992**, *46*, 9002.

[18] Afflek, I.; Kennedy, T.; Lieb, E. H.; Tasaki, H. *Phys. Rev. Lett.* **1987**, *59*, 799.

[19] Tsvelik, A. M. *Phys. Rev. B: Condens. Matter* **1990**, *42*, 10499.

[20] Hosokoshi, Y.; Takizawa, K.; Nakano, H.; Goto, T.; Takahashi, M.; Inoue, K. *J. Magn. Magn. Mater.* **1998**, *177*, 634.

[21] Rajendiran, T. M.; Kahn, O.; Golhen, S.; Ouahab, L.; Honda, Z.; Katsumata, K. *Inorg. Chem.* **1998**, *37*, 5693.

[22] (a) Darriet, J.; Regnault, L. P. *Solid State Commun.* **1993**, *86*, 409. (b) Imanaka, Y.; Miura, N.; Nojiri, H.; Luther, S.; Ortenberg, M. V.; Yokoo, T.; Akimitsu, J. *Physica B* **1998**, *246*, 561. (c) Kimura, S.; Ohta, H.; Motokawa, M.; Yokoo, T.; Akimitsu, J. *J. Magn. Magn. Mater.* **1998**, *177*, 624. (d) Kimura, S.; Ohta, H.; Motokawa, M.; Yokoo, T.; Akimitsu, J. *J. Phys. Soc. Jpn.* **1998**, *67*, 2514. (e) Maiti, K.; Sarma, D. D. *Phys. Rev. B: Condens. Matter* **1998**, *58*, 9746. (f) Okubo, S.; Hayashi, M.; Ohta, H.; Motokawa, M.; Kikuchi, H.; Nagasawa, H.; Kitamura, N. *J. Magn. Magn. Mater.* **1998**, *177*, 763. (g) Penc, K.; Shiba, H. *Phys. Rev. B: Condens. Matter* **1995**, *52*, R715. (h) Zheludev, A. *Physica B* **1997**, *241*, 495. (i) Zheludev, A.; Ressouche, E.; Maslov, S.; Yokoo, T.; Raymond, S.; Akimitsu, J. *Phys. Rev. Lett.* **1998**, *80*, 3630.

[23] Brunel, L. C.; Brill, T. M.; Zaliznayak, I.; Boucher, J. P.; Renard, J. P. *Phys. Rev. Lett.* **1992**, *69*, 1699.

[24] Bencini, A.; Gatteschi, D. *EPR of Exchange Coupled Systems*; Springer: Berlin, 1990.

[25] (a) Bencini, A.; Gatteschi, D. *Transition Metal Chemistry* **1982**, *8*, 1. (b) Goodman, B. A.; Raynor, J. B. *Advances in Inorganic Chemistry and Radiochemistry* **1970**, *13*, 136. (c) McGarvey, B. R. *Transition Met. Chem.* **1966**, *3*, 89. (d) Rubins, R. S.; Clark, J. D.; Jani, S. K. *J. Chem. Phys.* **1977**, *67*, 893. (e) Van Dam, P. J.; Klaassen, A. A. K.; Reijerse, E. J.; Hagen, W. R. *J. Magn. Reson.* **1998**, *130*, 140.

[26] Jimenez, H. R.; Salgado, J.; Moratal, J. M.; Morgenstern-Badarau, I. *Inorg. Chem.* **1996**, *35*, 2737.

[27] Li, S.; Hamrick, Y. M.; van Zee, R. J.; Weltner, W., Jr. *J. Am. Chem. Soc.* **1992**, *114*, 4433.

[28] (a) Barra, A. L.; Brunel, L. C.; Gatteschi, D.; Pardi, L.; Sessoli, R. *Acc. Chem. Res.* **1998**, *31*, 460. (b) Barra, A. L.; Caneschi, A.; Gatteschi, D.; Sessoli, R. *J. Am. Chem. Soc.* **1995**, *117*, 8855. (c) Barra, A. L.; Caneschi, A.; Gatteschi, D.; Sessoli, R. *J. Magn. Magn. Mater.* **1998**, *177*, 709. (d) Barra, A. L.; Gatteschi, D.; Sessoli, R. *Phys. Rev. B: Condens. Matter* **1997**, *56*, 8192−8198. (e) Dei, A.; Gatteschi, D.; Pardi, L.; Barra, A. L.; Brunel, L. C. *Chem. Phys. Lett.* **1990**, *175*, 589. (f) Goldberg, D. P.; Telser, J.; Krzystek, J.; Montalban, A. G.; Brunel, L. C.; Barret, A. G. M.; Hoffman, B. M. *J. Am. Chem. Soc.* **1997**, *119*, 8722. (g) Telser, J.; Pardi, L. A.; Krzystek, J.; Brunel, L.-C. *Inorg. Chem.* **1998**, *37*, 7, 5769.

[29] van Kralingen, C. G.; van Ooijen, J. A. C.; Reedijk, J. *Transition Met. Chem.* **1978**, *3*, 90.

[30] Ajiro, Y.; Asano, T.; Fumimori, M.; Mekata, M.; Aruga-Katori, H.; Goto, T.; Kikuchi, H. *Phys. Rev. B: Condens. Matter* **1995**, *51*, 9399.

[31] Kikuchi, H.; Ajiro, Y.; Mori, N.; Goto, T.; Aruga, I. *Solid State Commun.* **1990**, *76*, 999.

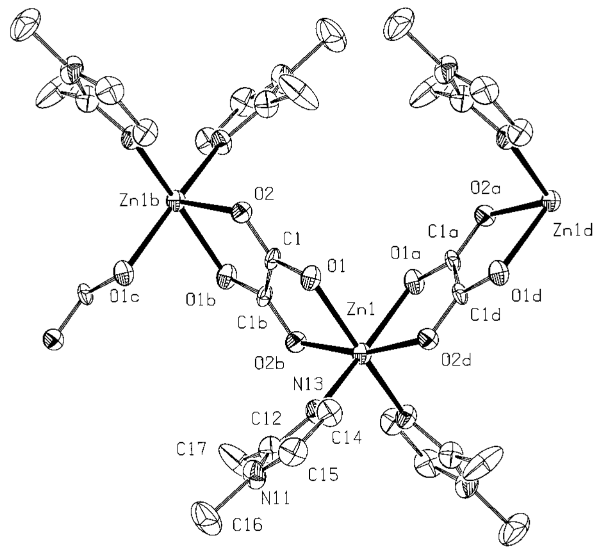

Figure 1. ORTEP projection (at 50% probability) of the molecular structure of the Zn/Ni(ox)(dmiz)$_2$ synthesized with 7% Ni; only part of the zigzag chain is shown.

of the Ni(II) ion in a Haldane system. To make sure that the structure of the Haldane system is the same as that of the parent compounds, an X-ray structure was determined.

Experimental Section

Synthesis. In a typical synthesis, 0.647 g (4.75 mmol) of anhydrous zinc chloride and 0.059 g (0.25 mmol) of $NiCl_2(H_2O)_4$ were dissolved in 40 mL water, and 1.923 g (20 mmol) of dmiz was added to this solution. This mixture was heated to 100 °C and stirred. Adding 0.670 g (5 mmol) of sodium oxalate in 40 mL of hot water (100 °C) to this metal-containing solution at 100 °C resulted in the formation of an oxalate complex solution. After filtration through a 589^3 blue ribbon ashless filter paper (S&S), a clear solution was obtained. Crystallization of the complex started spontaneously by cooling slowly to room temperature. Nice thin colorless needle-formed crystals were obtained. Mixtures of zinc(II) and nickel(II) chlorides in different ratios were used to obtain the mixed-metal complexes. The molar ratio between the metals nickel and zinc was obtained in each case by atomic absorption spectroscopic analysis. The sample $[Zn_{0.93}Ni_{0.07}(C_2O_4)(dmiz)_2]$ was used for a crystal structure determination.

Magnetic Measurements. All the EPR spectra were recorded with the EPR spectrometers of the EMR facility at the National High Magnetic Field Laboratory. The spectrometer is equipped with a superconducting Oxford magnet which can be continuously swept from 0 T to the maximum operating field of 17 T. A continuous flow cryostat allows a temperature control on the sample from room temperature down to 1.6 K. The microwave source is an Gunn diode (ABmm, Paris) emitting at a basic frequency of (110 ± 3) GHz, equipped with a harmonic generator that provides higher harmonics of the fundamental frequency. Detailed information is found elsewhere.[32]

EPR powder spectra were recorded in the frequency range from 110 to 440 GHz, and in the temperature range from 280 to 4.2 K. As a preliminary investigation X-band spectra were recorded with a Bruker 109 ESR in the 0−0.6 T magnetic field range and from room temperature to liquid helium temperature. All samples were EPR silent in these frequency, field, and temperature ranges. The high-field spectra were recorded on both loose and pelleted powders. Orientation effects in the magnetic field were consistently observed in the loose powder spectra, notwithstanding the low concentration of the Ni ion.[28b,33]

X-ray Structure Determination and Refinement. X-ray data were collected, using the inert oil technique, on an Enraf-Nonius CAD4T/rotating anode diffractometer for a light blue needle-shaped crystal. The structure was solved with Patterson techniques (DIRDIF[34]) and refined on F^2 by full-matrix least-squares techniques (SHELXL97).[35] Hydrogen atoms were introduced at calculated positions and refined riding on their carrier atoms. Correction for absorption was considered unnecessary. A final difference Fourier map did not show any excursions outside the region −0.66 and 0.66 e Å^{-3}. The Zn/Ni site was taken with 100% Zn occupancy in the final refinement. Basic data are given in Table 1, with detailed data in Table S1 of the Supporting Information.

Table 1. Crystal Data and Structure Refinement for the Derivative with $x = 0.07$

formula	$C_{12}H_{16}N_4O_4Zn$
fw	345.68
system	monoclinic
space group	$C2/c$ (No. 15)
a, Å	14.5252(7)
b, Å	12.1916(8)
c, Å	8.6850(8)
β, deg	97.460(6)
V, Å^3	1524.97(19)
Z	4
T, K	150
d_{calc}, g cm^{-3}	1.506
μ, mm^{-1}	1.6
radiation (λ, Å)	Mo Kα (0.71073)
R_1, wR_2, S	0.0733, 0.1388, 1.0

An exploratory population parameter refinement (with constrained position and displacement parameters), in order to establish the Ni/Zn ratio in the crystal, refined to 0.62(6)/0.38(6) Ni/Zn with a slight improvement of the R value (0.071). This ratio deviates significantly from the ratio (7/93) established by other methods (AAS) for the sample from the synthesized and used batch. Since it is not clear whether this is a refinement artifact in view of the small difference in scattering power between Zn and Ni, it was decided to base the results presented here on 100% Zn. Geometrical calculations and the ORTEP illustration were done with PLATON.[36]

Final atomic coordinates and thermal parameters are given in Tables S2−S4. Bonding information is given as Supporting Information in Tables S5−S9.

Results

Description of the Structure. The structure is as expected of the known type of zigzag chain. It contains distorted octahedrally coordinated metal ions with two cis-oriented N-coordinated dmiz ligands and two cis-oriented, tetradentate bridging oxalato(2−) ligands, together resulting in a MN_2O_4 donor set. Therefore, the structure differs from the hypothetical one reported in ref 31, in which a trans disposition of the oxalate molecules was assumed. In the refinement it was assumed that all metal ions are Zn and that the Ni(II) ions located at the Zn positions are randomly distributed. Metal−nitrogen distances are 2.098(5) Å and metal−oxygen distances are 2.168(5) Å. Other bond lengths are uneventful and are listed in Tables S3. Coordination angles are 78.4−100.7° for cis, with trans angles of 163.9 and 165.5°. Metal−metal distances in the chain are 5.513(1) Å, whereas the interchain metal−metal contacts are 8.685(1) Å. A picture of the molecular unit and part of the chain is shown in Figure 1. The packing in the crystal lattice is of van der Waals nature only.

---

(32) Hassan, A. K.; Pardi, L. A.; Krzystek J.; Sienkiewicz A.; Rohrer, M.; Goy, P.; Brunel, L.-C. *J. Magn. Reson.*, in press.

(33) Hulliger, J.; Zoller, L.; Ammeter, J. H. *J. Magn. Reson.* **1982**, *45*, 512.

(34) Beurskens, P. T.; Admiraal, G.; Beurskens, G.; Bosman, W. P.; Garcia-Granda, S.; Gould, R. O.; Smits, J. M. M.; Smykalla, C. The DIRDIF96 program system, Technical Report of the Crystallography Laboratory, University of Nijmegen, The Netherlands, 1992.

(35) Sheldrick, G. M. SHELXL97. Program for crystal structure refinement; University of Göttingen, Germany, 1997.

(36) Spek, A. L. *Acta Crystallogr.* **1990**, *A46*, C34.

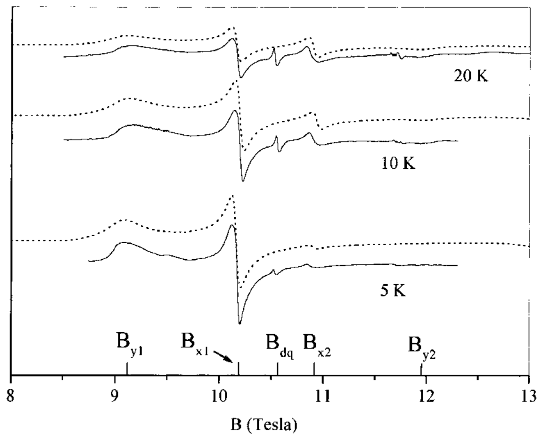

Figure 2. Temperature evolution of the 330 GHz EPR spectra of the title compound on blocked powders: (solid) experimental and (dashed) simulations, as described in the text. The different features are labeled according to the Wasserman notation.[38]

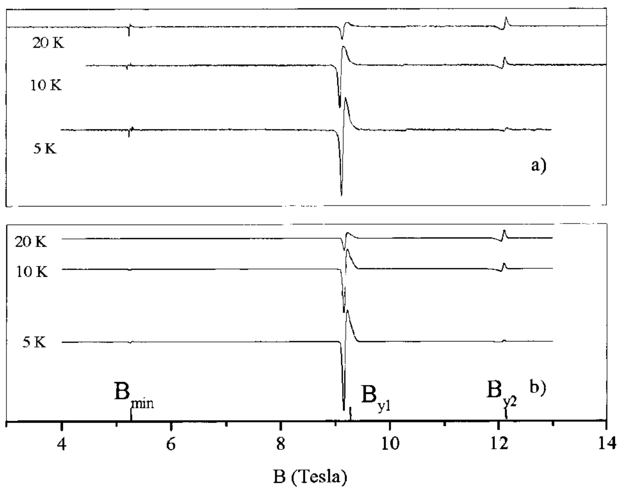

Figure 3. Temperature evolution of the 330 GHz EPR spectra on loose powders: (a) experimental and (b) simulations. The different features are labeled according to the Wasserman notation.[38]

High-Field EPR Study. EPR spectra at frequencies ranging from 110 to 440 GHz were recorded on loose powder and pellets of $Ni_xZn_{1-x}(C_2O_4)(dmiz)_2$ (dmiz = 1,2-dimethylimidazole) for $x = 0.09$ and 0.07. The two samples have identical EPR spectra and will not be distinguished in the following. They do not show any signals from room temperature down to 40 K at any of the used frequencies. At temperatures lower than 40 K, however, a series of signals starts to appear.

The temperature evolution of the 330 GHz spectrum of a pellet is shown in Figure 2. The fine structure shown in Figure 2 is reproducible at all the used frequencies, and the relative positions of the different transitions are independent of the frequency. The temperature dependence of the intensity of the various components of the spectrum is particularly evident in the loose powder spectra. Figure 3 shows the temperature evolution of the 330 GHz spectrum of the loose powders. At 40 K the amplitude ratio of the two main features is about 1:1, while at lower temperatures the high-field transition becomes less intense and almost vanishes at the lowest temperature.

A decrease of the intensity of the pellet spectrum compared to that of the loose powder is generally observed. This effect is attributed to an increase of lossiness due to reflection of the microwaves at the surface of the pellet. There is also a broadening of a part of the pellet spectrum compared to that of the loose powder, which is not presently well-understood. In particular, the features observed in the loose powder at 9.1 and 12.0 T are broadened in the pellet spectrum.

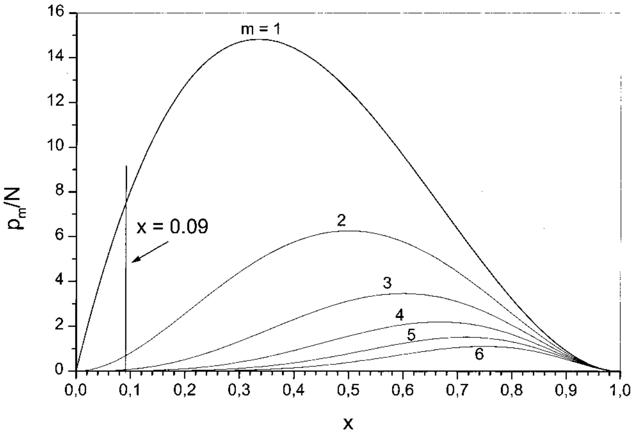

Figure 4. Calculated percentage of Ni(II) clusters of different nuclearity (m) in the Zn chain as a function of the fractional percentage, x. The vertical line corresponds to $x = 0.09$.

Spectra were performed on the same pellet after 6 months from the first spectrum and the broadening was clearly reduced. This observation points to strain induced in the lattice by the pressure applied to make the pellet. Another comparison between the spectra of the loose powders and the pellets shows that orientation effects[33] are clearly operative in the loose powders. In the spectra of both the loose powders and the pellets, half-field transitions (hft) are observed. These are forbidden ($\Delta M_s = \pm 2$) transitions. They show a marked and well-resolved anisotropy. Another signal is present around $g = 2$ at all frequencies. This signal is attributed to the double quantum transition. Recently, an unusual behavior of the intensity of the double quantum transition was reported,[25e] but no attempts were made in the present study to measure the intensity dependence on the incident power of this transition.

Discussion

Doping Ni^{2+} into the Zn chains creates a statistical distribution of isolated ions (monomers), dimers, trimers, etc. in the system. The distribution of these linear clusters depends on the fractional percentage of Ni ions added to the system. The appropriate statistic, assuming a random distribution, is given by the following formula (after Amoretti),[37]

$$P_m = N(1 - x)^2 x^m \tag{2}$$

which gives the probability (p_m) to find a cluster of m consecutive Ni(II) ions as a function of the fractional percentage (x) of Ni^{2+}, that is the number of Ni^{2+} ions over the total number (N) of atoms in the chain.

The calculated probabilities reported in Figure 4 clearly show that at percentages lower than 0.10 the isolated Ni^{2+} ions are statistically prevailing. The observed EPR spectra are thus assigned to the $S = 1$ Ni^{2+} ions split in zero field by single-ion anisotropy.

The fine structure shown in Figures 2 and 3 is attributed to a spin triplet with a large rhombic distortion. The two features observed at 9.1 and ~12.0 T in the loose powder spectrum performed at 330 GHz correspond to the transition parallel to the easy direction of the magnetization of the system. This is in turn determined by the magnetic anisotropy of the Ni(II) ions.

---

(37) Amoretti, G.; Buluggiu, E.; Vera, A.; Calestani, G.; Mattacotta, F. C. *Zeitschrift Fur Physik B—Condensed Matter* **1998**, *72*, 17.

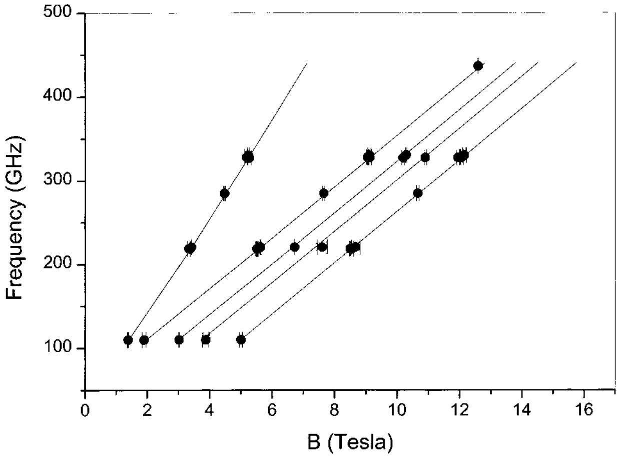

Figure 5. Frequencies vs observed transition fields for compounds with $x = 0.07$ and $x = 0.09$. The lines correspond to the canonical transition fields calculated with the Wasserman equations[38] adjusting the spin Hamiltonian parameters to fit the observed transitions (see the text). Multiple points correspond to different experiments at slightly different frequencies.

The hft transitions are very useful for two reasons: (i) they show up very easily because of their small anisotropy and (ii) they give a good first estimate of the zfs parameters.

Calculation of the transition fields using the formulas of Wasserman[38] allowed us to start the simulation process with a relatively good guess of the spin Hamiltonian parameters. Fitting of the transition fields was performed using a standard minimization procedure based on the Levenberg–Marquardt method[39] for all the observed spectra. The result of the fitting is graphically reported as a frequency vs field plot in Figure 5. The experimental points are the transitions observed at frequencies ranging from 110 to 440 GHz. The spin Hamiltonian parameters obtained from this fit are $g_x = 2.222(1)$, $g_y = 2.216(1)$, $D = 1.875(2)$ cm^{-1}, and $E = 0.38(4)$ cm^{-1} for an $R = 5 \times 10^{-4}$ (see below for the estimation of the g_z). Simulation of the spectra at 330 GHz[40] with these parameters at the different temperatures is shown in Figure 2 for different temperatures.

In the simulation of the pellet spectra an anisotropy of the line width was allowed and gave a satisfactory agreement with the experiment. The line widths were 0.1 T along the x and z axes and 0.05 T along the y axis. Such large anisotropy in the line width is evident in the pellet spectra. This phenomenon can be tentatively attributed to g or D strain, or both. The fact that the z direction could not be clearly observed is due to the fact that it is broadened beyond the level of observation in the pellet. Thus the g_z could not be determined. The only guess concerning g_z could be made on the basis of the crystal field requirements imposed by eq 3:

$$D = \frac{\lambda}{2}\left[g_z - \frac{1}{2}(g_x + g_y)\right]$$
$$E = \frac{\lambda}{4}(g_x - g_y) \qquad (3)$$

where $\lambda = \pm\xi/2S$, and ξ is the one-electron spin–orbit coupling constant that can be taken as 603 cm^{-1} for divalent nickel.[25c] Using eq 3 as a constraint in the fitting procedure leading to Figure 5, we obtain $g_x = 2.220$, $g_y = 2.215$, $g_z = 2.230$, $D = 1.868(4)$ cm^{-1}, and $E = 0.38(1)$ cm^{-1}, $R = 6 \times 10^{-4}$, in good agreement with the above calculations. Simulations were also performed to reproduce the spectra of the oriented samples. They are reported in Figure 3, together with the experimental spectra. The spectra of Figure 3b are calculated by assuming that the crystallites are oriented in a cone of 10° aperture along the y axis. Despite this crude assumption the temperature dependence and the position of the resonances are very well-reproduced. The intensity of the hft is not well-reproduced. The reason for this is that the simulation program we use[40] does not allow different line widths for different transitions, which would be desirable. The agreement between the spin Hamiltonian parameters obtained from all the calculations reported in Figures 2–5, confirms the validity of the model.

Table 2. Spin Hamiltonian Parameters for Selected Six-Coordinate Ni(II) Complexes

compounds[a]	chromophore	g_{av}	D (cm^{-1})	D/E	ref
$NiSO_4{\cdot}6H_2O$	NiO_6	2.25	4.85	0.01	41a
$(Fe,Ni)SiF_6{\cdot}6H_2O)$	NiO_6	2.26	−3.1	0.056	41b
$Ni(BrO_3)_2{\cdot}6H_2O$	NiO_6	2.29	−2	0	41c
$(Zn,Ni)SiF_6{\cdot}6H_2O)$	NiO_6	2.26	−0.6	0	41d
$[Ni(Him)_6](NO_3)_2$	NiN_6	2.19	0.88	0	41e
$[Ni(Him)_6](ClO_4)_2$	NiN_6	2.2	0.46	0	41f
$[Ni(Hpz)_6](NO_3)_2$	NiN_6	2.19	0.1	0.001	41f

[a] Abbreviations: Him, imidazole; HPz, pyrazole.

Six-coordinate Ni(II) complexes show a large interval of D and E values depending, as expected, on the donor set as well as on the coordination geometry of the complex. Complexes with oxygen donors (donor set NiO_6) have D values ranging from a fraction of a wavenumber to some wavenumbers. The nitrogen donors complexes have generally lower values of the anisotropy, with D lower than 1 cm^{-1}. The spin Hamiltonian parameters determined by EPR spectroscopy for some selected complexes taken from literature[41,42] are reported in Table 2. It is worth noting that the D value observed in the title complex is intermediate between those of the NiN_6 and of the NiO_6 chromophore, as would be expected from the NiN_2O_4 donor set. This coordination geometry has not been investigated before and thus a comparison cannot be made. Work is in progress to calculate the zfs parameters from first principles using an angular overlap model.

Concluding Remarks

The high-field/high-frequency EPR spectra of $Ni_xZn_{1-x}(C_2O_4)(dmiz)_2$ with moderate values of the Ni doping level x ($x = 0.07$, 0.09) show a series of signals attributed to isolated Ni(II) ions in the zinc chains. They are interpreted as the spectra of a spin triplet with a rhombic zfs ($E/D = 0.2$). The environment of the Ni ions is distorted octahedral and the spectra reveal a tetragonal distortion, as would be expected on the basis of the geometry of the chromophore. Previous works[29–31] have determined the size of the exchange coupling constant J and the value of the energy gap of $Ni(C_2O_4)(dmiz)_2$, as 29.8 and 13.2 cm^{-1}, respectively. The observation of a zfs on the order

---

(38) Wasserman, E.; Snyder, L. C.; Yager, W. A. *J. Chem. Phys.* **1964**, *41*, 1763.

(39) Press: W. H.; Flannery, B. P.; Teukolsky, S. A.; Vettering, W. T. *Numerical Recipes. The Art of Scientific Computing*; Cambridge University Press: Cambridge, 1986.

(40) Glerup, J.; Weihe, H. *Acta Chem. Scand.* **1991**, 444.

(41) (a) Pontuschka, W. M.; Piccini, A.; Quadros, C. J. A.; Isotani, S. *Phys. Lett.* **1973**, *44*A, 57. (b) Rubins, R. S. *J. Chem. Phys.* **1974**, *60*, 4189. (c) Suassuna, J. F.; Rettori, C.; Vargas, H.; Barberis, G. E.; Hennies, C. E.; Oliveira, N. F., Jr. *J. Phys. Chem. Solids* **1977**, *38*, 1075. (d) Rubins, R. S.; Jani, S. K. *J. Chem. Phys.* **1977**, *66*, 3297. (e) Sczaniecki, P. B.; Lesiak, J. *J. Magn. Reson.* **1982**, *46*, 185. (f) Reedijk, J.; Nieuwenhuijse, B. *Rec. Trav. Chim.* **1972**, *91*, 533.

(42) Brill, T. M.; Boucher, J. P.; Brunel, L. C.; Renard, J. P.; Verdaguer, M. *Physica B* **1995**, *204*, 303.

of 10% of the energy gap changes the estimation but maintains the assignment of this system to the class of Heisenberg antiferromagnets. This is very important because the interpretation of the magnetization data would need a different approach[43] would the Ni(II) ion anisotropy be on the order of 10 cm^{-1} or higher.[26,27]

Taking advantage of the already mentioned fact that in $Ni(C_2O_4)(dmiz)_2$ the nickel ions can be substituted with zinc ions in any desired ratio, we are trying to establish the minimum doping level necessary to start to observe the Haldane behavior. That would be, for example, monitored by observing the EPR transitions observed in other Haldane systems[12,23,42] and/or by the observation of the assignment of this $s = {}^1/_2$ Haldane system at the end of the chains.[5,9,44] The latter are effects due to the finite size of the chains in the sample or, in other word, the termination of the chains. They are revealed by the appearance of new signals in the EPR spectra which are expected to be well-separated from those described in this work.

Acknowledgment. The authors are indebted to the EU for a grant as Host Institute in the EU Program Human Capital and Mobility (1994−1997). This work has been supported by the Leiden University Study group WFMO (Werkgroep Fundamenteel-Materialen Onderzoek) which is kindly acknowledged, and by the Chemical Research Council of The Netherlands. Thanks are due to the Human Frontier Science Program (RG-349/94 to L.-C. B.) and to the NHMFL (L.A.P. and L.-C. B.). L.A.P. wants to acknowledge support from the Conzortio INSTM. Prof. Dante Gatteschi is thanked for critical reading of the manuscript.

Supporting Information Available: X-ray crystallographic data. This material is available free of charge via the Internet at http://pubs.acs.org.

IC990167X

---

(43) Golinelli, O.; Jolicoeur, Th.; Lacaze, R.; *Phys. Rev. B: Condens. Matter* **1992**, *46*, 10854.

(44) Glarum, S. H.; Geschwind, S.; Lee, K. M.; Kaplan, M. L.; Michel, J. *Phys. Rev. Lett.* **1991**, *67*, 1614−1618.